Resveratrol improves TNF-α-induced endothelial dysfunction in a co-culture model of a Caco-2 with an endothelial cell line

Isabela Maia Toaldo[a,b], John Van Camp[b], Gerard Bryan Gonzales[b], Senem Kamiloglu[b,e], Marilde T. Bordignon-Luiz[a], Guy Smagghe[c], Katleen Raes[d], Esra Capanoglu[e], Charlotte Grootaert[b*]

[a]Department of Food Science and Technology, Federal University of Santa Catarina, Admar Gonzaga 1346, 88034001 Florianópolis, Brazil

[b]Department of Food Safety and Food Quality, Ghent University, Coupure Links 653, 9000 Gent, Belgium

[c]Department of Crop Protection, Faculty of Bioscience Engineering, Ghent University, Coupure Links 653, 9000 Gent, Belgium

[d]Department of Industrial Biological Sciences, Faculty of Bioscience Engineering, Ghent University, Graaf Karel de Goedelaan 5, 8500 Kortrijk, Belgium

[e]Department of Food Engineering, Faculty of Chemical and Metallurgical Engineering, Istanbul Technical University, 34469 Maslak, Istanbul, Turkey.

***Present address:** Dr. ir. Charlotte Grootaert, Department of Food Safety and Food Quality, Ghent University, Coupure Links 653, 9000 Gent, Belgium. **E-mail address:** charlotte.grootaert@ugent.be. **Tel./Fax:** +32-(0)9 264 62 08.

Abbreviations:

eNOS, endothelial nitric oxide synthase; ICAM-1, intercellular adhesion molecule-1; IFN-γ, interferon γ; IL-1, interleukin-1; IL-8, interleukin-8; KDR, tyrosine kinase receptor; NF-*κ*B, transcription nuclear factor *κβ*; NO, nitric oxide; ; Romo1, ROS modulator; ROS, reactive oxygen species; RSV, *trans*-resveratrol; TNF-*α*, tumor necrosis factor *α*; VASP, vasodilator-activated protein; VEGF, vascular endothelial growth factor.

Chemical compounds studied in this article

trans-resveratrol (PubChem CID: 445154)

interleukin-8 (PubChem CID: 44357137)

Abstract

The bioactivity of *trans*-Resveratrol (RSV), an important wine polyphenol, and of its metabolites was investigated in a more relevant setup comprising an *in vitro* co-culture cell model that combines intestinal absorption and conjugation with changes in endothelial function, which is primarily affected in cardiovascular diseases. Caco-2 and endothelial EA.hy926 cells were grown in a co-culture and Caco-2 cells were treated with RSV, in the co-culture and in two different sequential setups, for 4 h and 24 h. Transported metabolites were investigated by UPLC-MS/MS^{E} and the effects on NO production, ROS inhibition and secretion of vascular endothelial growth factor (VEGF), interleukin-8 (IL-8) and intercellular adhesion molecule-1 (ICAM-1) were evaluated in TNF-α-activated and non-activated endothelial cells. RSV and four conjugated metabolites, two sulfates and two glucuronides, were identified after intestinal transport. In both co-culture and sequential systems, RSV at 20 µM strongly induced NO production. Changes in ROS and NO levels demonstrated a clear effect of crosstalk between cells in the co-culture. The secretion of proinflammatory cytokines and VEGF was largely increased by treatment with TNF-α (inflammatory condition). The polyphenol intervention significantly reduced the levels of VEGF, ROS, IL-8 and ICAM-1, with a more pronounced effect in TNF-α-activated endothelial cells. In conclusion, RSV and its metabolites showed accentuated bioactivity on TNF-α-induced inflammation and the metabolism of endothelial cells as a biological target was not only influenced by these phenolics, but also by the communication between distinct cell lines, showing a new perspective for investigations on polyphenol intervention and its biological outcomes.

Keywords: Cardiovascular disease; Co-culture; ICAM-1; Intestine; Nitric oxide; Resveratrol

1 Introduction

Cardiovascular diseases are the leading cause of death and disability in the Western world and include several pathological conditions related to dysfunction of blood vessels, including arteries, veins and capillaries [1]. Atherosclerosis is a chronic inflammatory disease characterized by the formation of atherosclerotic plaques (atheromas), caused by endothelial injury and vascular wall inflammation that trigger the accumulation of oxidized lipid molecules, infiltration of macrophages, lymphocytes and connective tissue components, and the proliferation of smooth muscle cells [1,2].

Oxidative stress and inflammation in endothelial cells are intimately associated with the development of atherosclerosis. Reactive oxygen species (ROS) act as potent oxidants of key biological molecules causing impairment of various cellular functions. In the endothelium, the activation of the transcription nuclear factor NF-κB and proinflammatory cytokines such as tumor necrosis factor α (TNF-α), interleukin-1 (IL-1), interleukin-8 (IL-8) and interferon γ (IFN)-γ accelerates atheroma formation [3,4]. Additionally to inflammation and oxidation, the pre-events in atherosclerosis include metabolic conditions such as dyslipidemias, hypertension, diabetes and obesity, and lifestyle changes and dietary habits comprise important factors to counteract oxidative damage and inflammation [5].

The consumption of polyphenol-rich diets is associated with a reduced risk of chronic diseases. Grape derivatives such as wine and grape juice are highly appreciated worldwide and account for one of the most important sources of polyphenols in the human diet [6]. Resveratrol (*trans*-3,5,4′-trihydroxystilbene; RSV) is an important bioactive stilbene present in grapes, red wine and berries, with health-related properties towards cardiovascular functions [7,8]. Both *in vivo* and *in vitro* research has demonstrated the potential of RSV to modulate angiogenesis [9], cell signaling [10], markers for vasorelaxation [11], expression of

inflammatory factors and adhesion molecules [12,13] and gene transcription [14]. However, RSV is strongly metabolized to glucuronated and sulfated metabolites by mostly intestine and liver [15], and especially glucuronides were shown to be less bioactive *in vitro* [16]. So far, mechanistic studies have not included the excessive RSV metabolism during intestinal absorption in their design, and crosstalk mechanisms between different cell types as an indirect result of RSV addition are often overlooked. Yet, these mechanisms are of importance because the crosstalk between gut epithelial cells and endothelium involves triggering of signaling pathways of immune and inflammation responses, which are key modulators of endothelial dysfunction [17,18].

In this work, we have evaluated the use of an *in vitro* co-culture model combining absorption effects with changes in endothelial function for the investigation of cellular responses after RSV treatment. Oxidative stress and the secretion of endothelial markers were evaluated under inflammatory and non-inflammatory conditions induced by TNF-α. In addition, shifts in RSV metabolism were investigated using LC-MS/MS^E and correlated with the observed bioactive effects.

2 Materials and Methods

2.1 Cell lines and cell culture

The experiments were performed using the continuous cell line Caco-2 (HTB-37™, ATCC, Manassas, VA, USA), which differentiates into enterocyte-like cells upon confluency, and the permanent human endothelial cell line EAhy926 (CRL2922™, ATCC). This endothelial cell line was chosen because of its continuous character, resulting in a fast and constant growth rate and more consistent response compared to primary cell lines such as

HUVEC. The Caco-2 cells (passage 15–27) and endothelial cells (passage 9–15) were grown separately as adherent cultures in 25 cm^2 tissue culture flasks (Sarstedt, Essen, Belgium) and cultivated in Dulbecco's modified Eagle's growth medium (DMEM), high glucose, supplemented with glutamax™, sodium pyruvate, 10% (v/v) fetal bovine serum (Greiner bio-one, Wemmel, Belgium), penicillin (100 U/ml), and streptomycin (100mg/ml) (Gibco, Life Technologies, Ninove, Belgium). Cells were subcultured once a week with 0.25% (v/v) trypsin-EDTA and grown until 90% confluence. The culture medium was replaced every other day. Cells were incubated at 37 ºC and 10% CO_2 in a water saturated atmosphere.

2.2 Assays for mitochondrial activity

Cellular mitochondrial activity after treatment with *trans*-resveratrol (RSV, 99% purity) (Sigma-Aldrich, St. Louis, MO, USA) was measured using the MTT assay (3-[4,5-dimethylthiazol-2-yl]-2,5 diphenyl tetrazolium bromide) (Sigma-Aldrich), as previously described [19]. Caco-2 and endothelial cells were seeded in 96-well plates at a concentration of 20,000 cells per well. Upon 100% confluency, cells were treated with serum-free exposure medium spiked with RSV at a concentration range of 1-100 μM and incubated at 37 °C, 10% CO_2. The MTT test was performed after 3-days treatment for differentiated Caco-2 cells and 2-days treatment for endothelial cells. Absorbance was measured at 570 nm using a Bio-Rad multiplate reader (Bio-Rad Laboratories, Hercules, CA, USA). Results are expressed as % of mitochondrial activity compared to untreated cells.

2.3 Experimental setup: co-culture, sequential and standard culture

Three types of experimental setups were used: (i) co-culture of Caco-2 cells with EA.hy926 cells, (ii) sequential culture of Caco-2 cells with EA.hy926 cells and (iii) standard culture which is a monoculture of EA.hy629 cells. (i) For the co-culture setup, Caco-2 cells were seeded on 12-well Transwell plates (0.4 μm pore diameter, Elscolab, Kruibeke, Belgium) at a concentration of 250,000 cells per well. Fifteen days after confluency of the Caco-2 cells, EA.hy926 cells were seeded on the basolateral compartment of the Transwell plate, at a cell density of 300,000 cells per well. The EA.hy926 cells were grown in the co-culture system until they reached confluency on the third day. On the fourth day of co-culture, Caco-2 cells were treated apically with RSV in phenol-red free and serum-free exposure medium at concentrations of 5 μM and 20 μM, and RSV-free exposure medium was applied in the basolateral compartment. A concentration of 5 μM was chosen because it is in the same range of peak plasma concentrations after moderate wine and juice consumption as reported previously [20-22], and consequently, 20 μM is expected to be in the range of concentrations to which the gut epithelium is exposed to. Prior to RSV treatment, the basolateral compartment in the co-culture was incubated for 1 h with 10 ng/ml TNF-α in exposure medium in order to induce the high-grade inflammation associated with cardiovascular diseases. The co-culture was incubated at 37°C at 10% CO_2 and samples of culture medium of apical and basal compartments were collected after 4 h, to study short term effects [18], and after 24 h – to observe longer term effects – and immediately stored at -80 °C prior to analysis.

(ii) Additionally, the same set of experiments was performed in a sequential setup to investigate the effects of RSV on cellular responses in an isolated system. For the sequential setup, Caco-2 cells were cultivated on Transwell inserts and allowed to differentiate for 15 days after confluency, and EA.hy926 cells were seeded in a separate 24-well plate at a concentration of 100,000 cells per well. Prior to treatment at confluency, the endothelial cells

were treated with or without TNF-α as described before. EA.hy926 cells were incubated overnight either with the basolateral (transported) fraction collected at time points of 4 h and 24 h after RSV treatment of Caco-2 cells or with RSV standard solutions in exposure medium (5 μM and 20 μM). (iii) In the standard setup, only endothelial cells were pretreated with TNF-α and incubated with the RSV standard solutions.

2.4 Lucifer Yellow permeability test and TEER measurement

For all transport experiments, the apparent permeability coefficient (P_{app}) of Caco-2 cell monolayers were monitored before and after the experiments using the fluorescent reagent Lucifer yellow (Sigma-Aldrich, Diegem, Belgium) as a indicative marker of passive paracellular diffusion [23]. In addition, the integrity of the Caco-2 cell monolayer was monitored before and after the experiments using transepithelial electrical resistance (TEER) measurements with an automated tissue resistance measurement system (REMS, World Precision Instruments, Hertfordshire, UK). Only intact Caco-2 monolayers with TEER values of 900-1100 Ω cm^2 were used for the co-culture experiments.

2.5 High resolution mass spectrometry analysis (UPLC-HDMS/MS^E) analysis of resveratrol metabolites

LC-MS/MS analysis was performed with a Waters Acquity UPLC system (Waters Corp., Milford, MA, USA) connected to a Synapt HDMS TOF mass spectrometer (Waters Corp.). LC separation was done on a Waters Acquity BEHC18 column (2.1 mm × 150 mm, 1.7 m particle size) using gradient elution composed of (A) water (0.1% (v/v) formic acid) and (B) methanol (0.1% (v/v) formic acid) as earlier described [24]. The eluent was then

directed to the mass spectrometer equipped with electrospray ionization (ESI) source. Data were acquired in continuum negative ionization in V-mode. For MS/MS analysis, collision energies were set at 6 V for the low energy and 45 V for high energy. Mass range was set at 100–1500 Da with a scan speed of 0.2 s per scan using the MassLynx software 4.1 (Waters Corp.). Metabolynx™, which was embedded within the MassLynx package was used to perform automated peak detection and identification of phase I and II metabolites.

2.6 Determination of intracellular reactive oxygen species (ROS)

The inhibition of intracellular ROS was monitored in endothelial cells through the reaction with the oxidant sensitive fluorogenic probe H_2-DCFDA (2,7-dichlorodihydrofluorescein diacetate) (Sigma-Aldrich, St. Louis, MO, USA). The non-fluorogenic compound is converted by intracellular deacetylases to DCFH, which upon oxidation by ROS is converted to the highly fluorescent 2',7'-dichlorofluorescein (DCF) [25]. After the transport experiments with RSV at 5 μM and 20 μM, endothelial cells were incubated with 20 μM H2-DCFDA in exposure medium for 30 min. The cells were then washed with phosphate buffered saline (PBS) and lysed with cold ultrapure water 10% ethanol for 30 min. The samples were then centrifuged at 10000 x g for 10 min, and fluorescence of supernatants was immediately measured on a Spectramax Fluorescent Plate Reader ($\lambda_{ex/em}$=485/535 nm) (Molecular Devices, CA, USA).

2.7 Determination of nitric oxide (NO) production in endothelial cells

The production of NO in endothelial cells was monitored using the Griess colorimetric assay (Sigma-Aldrich), as previously described [9]. Concentrations of nitrite

(NO_2) were quantified through a six-point matrix-matched standard curve of sodium nitrite (NaNO2) (0-20 µmol/L). In the procedure, samples of culture medium were mixed with an equal volume of the Griess reagent. After 15 min at room temperature (18 °C), absorbance was read at 540 nm.

2.8 Determination of inflammation markers by enzyme-linked immunosorbent assays (ELISA)

The cellular secretion of IL-8, VEGF and ICAM-1 in the co-culture was determined in cell culture media collected at time points 4 h and 24 h from the basolateral compartment and analysed using the human IL-8 TMB, human VEGF TMB and human ICAM-1 ABTS ELISA kits (Peprotech, London, UK), respectively, following the manufacturer's instructions.

2.9 Statistical analysis

Data were analyzed using one-way analysis of variance (ANOVA) followed by Student's *t*-test to assess statistical differences from control values and between inflammatory and non-inflammatory conditions (Statistica 7.0 203, StatSoft Inc., Tulsa, USA). Statistical significance was regarded at $p<0.05$ or $p<0.001$. Results are expressed as mean ± standard error of mean (SEM). All experiments were carried out with three plates seeded at three different time points in the course of four months, comprising the biological replicates. For each biological replicate, results of three technical replicates were obtained.

3 Results

3.1 Identification of transported metabolites

The transport and metabolism of RSV by Caco-2 cells were tested in samples of basolateral media periodically collected between 0 h and 24 h. Upon 2 h exposure to 100 μM RSV, the presence of RSV and a hydrophilic metabolite was detected in the chromatogram. Upon further incubation, RSV and other three metabolites were detected after 24h incubation (data not shown). Hence, for the MS/MS^{E} analyses, the time point of 24 h was selected as optimized condition for identification of metabolites. Four monoconjugated metabolites were identified, comprising two sulfates and two glucuronides derivatives of RSV (Table 1). Fig. 1 shows the MS spectra and extracted ion chromatogram of a cell culture medium sample collected after 24 h incubation and transport by Caco-2 cells treated with 20 μM RSV.

In Fig. 1, MS data collected for RSV precursor and product ions shows the peaks of RSV and its main conjugated metabolites, confirmed based on the accurate mass of *m/z* transition and retention time (rt): *trans*-resveratrol (rt = 23.53), *trans*-resveratrol-4'-*O*-*β*-glucuronide (rt = 15.85), *trans*-resveratrol-4'-sulfate (rt = 17.23), *trans*-resveratrol-3-sulfate (rt = 20.19), *trans*-resveratrol-3-*O*-*β*-glucuronide (rt = 20.58). Although less abundant, the presence of an ion peak of RSV reveals that not only RSV conjugates, but also the polyphenol in its intact form, is transported by Caco-2 cells. The hydrophilic metabolites produced well-separated and well-defined peaks, at the retention time range of 15.0-21.0 min, with the highest intensity of sulfate metabolites. The MS spectra allowed a more accurate view of metabolites *m/z* transition, confirming the higher intensity of glucurono- and sulfo-conjugated derivatives in comparison with the parent compound. Also, the greater relative abundance of sulfated forms (*m/z* = 307.03) compared to the parent and glucuronide

ions revealed that sulfates are the main conjugates formed during Caco-2 metabolism of RSV.

3.2 Establishment of the co-culture characteristics and effect of RSV on cellular mitochondrial activity

To develop an *in vitro* model combining polyphenol absorption and effects on target tissue metabolism, differentiated Caco-2 cells were co-cultured with EA.hy926 cells and changes in permeability and cellular metabolism were monitored through mitochondrial activity in response to RSV in both TNF-α activated and non-activated cells. Regarding permeability, P_{app} values of apical-to-basolateral direction ranged from $4.61 \pm 0.25 \times 10^{-5}$ cm/s in the sequential system, composed of Caco-2 cells, to $4.80 \pm 0.23 \times 10^{-5}$ cm/s in the co-culture system, composed of Caco-2 cells and EAhy926 cells in apical and basolateral compartments, respectively. The TEER values ranged from $944.4 \pm 28.0\ \Omega\ cm^2$ in the sequential system to $1034.8 \pm 43.9\ \Omega\ cm^2$ in the co-culture. The integrity and permeability variables were negatively correlated and no significant difference was found between both systems ($p<0.05$). We can therefore conclude that co-culture of Caco-2 and EA.hy926 cells, as well as the TNF-α and RSV treatments, did not negatively affect the Caco-2 intestinal barrier integrity.

In contrast, changes in mitochondrial activity in response to RSV were largely influenced by cultivation method, with distinct responses observed in the co-culture, compared to sequential and standard culture methods (Fig. 2). A first observation is that only in the co-culture system after 24 h, the mitochondrial activity of TNF-α treated endothelial cells was significantly decreased by about 35% compared to the untreated cells, which was independent of RSV concentration. This effect was not visible in the sequential setup, where

only the endothelial cells have received the TNF-α treatment. Therefore, we may conclude that, upon TNF-α treatment, the Caco-2 cells secrete RSV-independent cytokines that damage the endothelium after 24 h.

A second observation is that under standard monoculture conditions, RSV increased mitochondrial activity in a dose-dependent way, which was most probably not the result of cell proliferation, as the total protein content of the wells, as measured with a sulforhodamin B (SRB) test, was not increased in parallel. The mitochondrial increase was not visible in the co-culture system, and also in the sequential setup no clear trend could be seen. This may be a first indication that native RSV, but not the transported conjugated metabolites, increases mitochondrial activity *in vitro*. Third, in general, trends of RSV treatment at different concentrations in the co-culture and sequential system after 4 and 24 hours are similar. More specifically, 5 µM RSV gave a slightly increased reactivity, whereas a slight decrease was observed at 20 µM. This observation illustrates that RSV induced cell signaling pathways may be concentration dependent. This reactivity was probably not related to apoptotic pathway induction, as in preliminary experiments, we verified that incubation of Caco-2 and EA.hy926 cells with similar RSV concentrations for three days did not result in cell toxicity.

3.3 NO production

The effect of RSV and its metabolites on cellular NO production is presented in Fig. 3. First, a 1-hour TNF-α pretreatment of cells resulted in significantly higher NO levels in the co-culture and sequential setup, especially after 24 h. Interestingly, this effect was not visible for the standard conditions. A second observation is that under standard as well as co-culture conditions, a concentration of 20 µM significantly increased NO production after 4 and 24 h of treatment with RSV, and in both TNF-α treated and untreated conditions. This is

consistent with literature for monoculture systems [9, 13]. However, at lower concentrations of RSV (5 μM), NO production was significantly reduced at 4 h and slightly reduced at 24 h, in the non-inflammatory condition.

Third, it could be observed that especially under TNF-*α* induced conditions, addition of RSV resulted in extra NO production in a dose-dependent way, but only in the co-culture and sequential setup. This may indicate that either the transported fraction containing RSV and its Caco-2 derived metabolites, rather than the polyphenol alone, improves NO production by the endothelial cells, or that NO is also produced by Caco-2 cells in response to RSV, or both.

3.4 RSV and metabolites inhibit oxidative stress in co-culture and sequential models

First, a one-hour treatment of the cells with TNF-*α* resulted in a strong increase in intracellular ROS in all setups, reaching 4-fold concentrations in the co-culture setup after 4 h (Fig. 4), which corresponds with literature data [18]. Secondly, when cells were pretreated with TNF-*α*, the increase in ROS was strongly dependent on the experimental setup. The fastest response was visible for the endothelial cells in the co-culture setup, as values were higher at 4 h compared to 24 h of incubation. The opposite was observed for the sequential setup, whereas the effect on standard monoculture setup was rather limited. Together with the MTT results, we conclude that the fast and strong oxidative response in the TNF-*α* stimulated co-culture setup has most probably led to permanent endothelial damage after 24 h caused by Caco-2 secreted factors.

Thirdly, the effect of RSV on ROS was dependent on both TNF-*α* treatment and experimental setup. Under non-inflammatory conditions, the effect of RSV was only significant in the co-culture model. At 5 μM RSV, intracellular levels of ROS were

significantly reduced after 4 h incubation, showing a late increase after 24 h incubation. For 20 μM RSV, the ROS levels in endothelial cells were consistently lower up to 24 h incubation in the co-culture model. Under inflammatory conditions, RSV treatment gave a dose-dependent decrease of ROS in the co-culture setup after 4 h, whereas the opposite was true for the sequential setup. After 24 h, this dose-response effect was less visible. These results indicate that addition of RSV in the co-culture setup may effectively reduce the oxidative stress induced in the endothelial cells by TNF-α and cytokines produced by the Caco-2 cells.

3.5 RSV affects inflammation markers in the co-culture

The secretion of proinflammatory markers was tested in both TNF-α-treated and untreated cells in order to determine RSV effects on endothelium responses under inflammatory and non-inflammatory conditions, respectively. Considering the results of oxidative parameters, we have chosen the co-culture model to study the influence of RSV on secretion of markers VEGF, ICAM-1 and IL-8. Changes in cytokine expression may therefore be caused by both cell types.

In TNF-α-activated cells, the secretion of markers was significantly higher in comparison with basal values of the non-inflammatory condition (Fig. 5), and increased concentrations of 1.5-fold up to 7-fold were verified for the adhesion ICAM-1 (107.10 pg/ml) and IL-8 (75.23 pg/ml) proteins, respectively. Concentrations of VEGF in the medium ranged from 12.06 to 236.44 pg/ml for untreated cells (blank) of the non-inflammatory and inflammatory conditions, respectively.

Under healthy conditions, the overall concentration of IL-8 (10.95 pg/ml) significantly decreased in a dose-dependent way in co-cultured cells treated with RSV at 5

μM (8.09 pg/ml) and 20 μM (9.40 pg/ml). Upon TNF-α activation, the secretion of IL-8 consistently reduced from 4 h to 24 h in cells exposed to RSV compared to the untreated cells. Remarkably, unlike VEGF and ICAM, the values of IL-8 under inflammatory conditions were higher after 4 hours compared to 24 h of treatment. These results indicate that, in contrast with the other tested chemokines, there was no constant accumulation of IL-8 in the medium over time, and that IL-8 may be bound to receptors, such as G-protein coupled receptors, which are present in both cell types [26,27]. Secondly, under normal conditions, RSV decreased VEGF secretion in a dose dependent way at 24h of treatment. Under TNF-α induced conditions, however, a dose-dependent increase of VEGF was observed after 4 h of treatment. After 24 hours, the trend was less visible. ICAM-1 expression significantly increased upon TNF-α stimulation. Interestingly, ICAM-1 was about 6-fold higher after 24 h of incubation, which corresponds with the time-point in which the mitochondrial activity of the endothelial cells was significantly reduced. Though some conditions showed an effect of RSV on ICAM-1 expression, no clear dose-dependent correlation could be observed.

4 Discussion

This study assessed the impact of *trans*-resveratrol and metabolites on key markers of mitochondrial activity, oxidative stress and inflammation associated with endothelial dysfunction in an *in vitro* cell culture setup that allowed intestinal metabolism and crosstalk between intestinal and endothelial cells. Though a similar co-culture model was developed recently [18], we have performed a more in-depth study on the value of our co-culture model compared to the conventionally used sequential and monoculture models. Besides this, major differences between the previously published model and the one discussed in this paper are

(i) the cell lines used for the co-culture, (ii) some of the biological endpoints, (iii) the use of resveratrol instead of a mixed grape anthocyanin extract and (iv) a detailed analysis of resveratrol metabolites that were actually reaching the endothelial cell compartment. When comparing our co-culture setup with the sequential and monoculture, evidence for crosstalk can be drawn from our results. Changes in ROS and NO levels in the co-culture demonstrated a clear effect of the communication between cell lines. Upon inflammation, the consistent decays on mitochondrial activity and intracellular ROS indicated damage of the endothelial cells due to oxidative mechanisms and the combined metabolism in the co-culture. This damage could be delayed by RSV, but not restored.

When comparing our co-culture model with the one previously reported [18], we have found some similarities. In fact, TNF-α exerted a strong inducible effect on the secretion of the adhesion molecule and proinflammatory chemokines in the co-culture. Also, this effect was more pronounced after the long-term incubation of 24 h. We evaluated RSV effects on secretion of VEGF, IL-8 and ICAM-1 in the co-culture model, in TNF-α-activated and non-activated cells. Diverse stimuli affecting NO regulation and ROS formation may lead to expression of these proinflammatory molecules in endothelium [28]. As expected, secretion of the endothelial growth factor, IL-8 cytokine and the adhesion molecule were largely increased by induction of inflammation with TNF-α. In fact, TNF-α modulates the expression of up to 4,000 genes in endothelial cells, most related to cell adhesion, inflammation and chemotaxis proteins [29]. We observed that upon exposure to TNF-α, levels of VEGF, NO and ROS were significantly increased in the co-culture. This effect may be explained by activation of mitochondrial Romo1 receptor, boosting ROS formation; and by upregulation of VEGF synthesis in endothelial cells, causing stimulation of the tyrosine kinase receptor VEGFR/Flt (KDR) involved in eNOS phosphorylation and NO activation [30,31]. In addition, VEGF, as well as IL-8 and ICAM-1 expression may be the result of

TNF-α-induced activation of NF-κB [32,33]. Despite the significant effect of RSV and its metabolites on reducing secretion of proinflammatory molecules in the co-culture, decreases on ICAM-1, VEGF and IL-8 concentrations in relation to each control were more pronounced in TNF-α-activated cells. Thus, suggesting that RSV and its metabolites operate through an inhibitory regulation of the inflammatory cascade in endothelial cells, which can maintain a more sustained effect under pre-existing inflammation.

Compared to the HUVEC cells in a co-culture [18], the EA.hy926 cell line used in this study has the advantage that it is an immortalized cell line with endothelial characteristics, and therefore are easy to cultivate without loss of growth and function over time. However, this cell line is the fusion product of primary umbilical vein cells with the A549 lung carcinoma cell line, and therefore, we can not rule out that some of the responses are driven by its cancerous origin. Yet, the co-culture system has the potential to mimic the *in vivo* conditions because of the following reasons; (i) the close proximity in a non-contact setup between the apical and basal cells mimicking the gut epithelial cells and target tissues; (ii) the Caco-2 cells in the apical compartment simulates the intestinal barrier as the first line of contact to the intestinal lumen in order to absorb dietary compounds; (iii) the direct communication between cell lines is affected by soluble mediators secreted by both cell types [17]. Therefore, we conclude that this model is able to study the impact of absorbed bioactive compounds on the endothelium.

Concerning the biological endpoints, we have studied endpoints of oxidative stress and inflammation. *In vivo*, this situation happens when there is an imbalance of oxidation mediators and antioxidant defenses [3,28]. Resveratrol has the potential to beneficially impact this situation [8,30]. In our results, RSV strongly influenced NO production in cells under healthy and unhealthy condition. Indeed, RSV has been reported to positively induce endothelial nitric oxide synthase (eNOS) activity and NO release in endothelial cells [34].

Resveratrol promotes NO activation through stimulation of phosphorylation of protein kinase B and vasodilator-activated protein (VASP) [11]. However, neither resveratrol sulfates nor glucuronides were able to induce NO release in endothelial cells [35]. Markedly, our results showed that ROS levels were only significantly reduced in the co-culture, after metabolism of RSV by Caco-2 cells.

During absorption, RSV undergoes excessive metabolism by gut epithelial cells, whereas only very low amounts of unconjugated resveratrol are circulating in the blood stream. The sulfated and glucuronated conjugates are present in larger amounts [8,36]. These conjugates were also found in our setup using LC-MS/MS, thereby confirming the value of using an intestinal cell culture in this *in vitro* study design. The MS analysis revealed four RSV conjugates produced through sulfation and glucuronidation processes of phase II metabolism by Caco-2, comprising two sulfate derivatives and two glucuronide metabolites. These are, in fact, the main metabolic conjugates of *trans*-resveratrol [36]. Moreover, endothelial cells treated with either the unconjugated polyphenol in the monoculture standard setup clearly behaved differently from the endothelial cells treated with basal medium after Caco-2 transport of RSV. This may be due to the low bioactivity of conjugated RSV metabolites as well as to other factors secreted by the Caco-2 cells during cellular metabolism. Indeed, previous literature suggest the low bioavailability of the parent polyphenol and lack of bioactivity of RSV metabolites [6,16]. Finally, no shifts in RSV metabolism as a result of TNF-α treatment could be observed, which indicates that the contact time of the endothelial cells with TNF-α was insufficient to induce crosstalk mechanisms that could regulate polyphenol uptake and metabolism by the cells.

5 Conclusions

This study demonstrated that RSV and its metabolites exert a protective effect in endothelial cells against oxidative stress and inflammation, which are intimately associated to cardiovascular diseases. This effect was verified in endothelial cells cultivated in both co-culture with intestinal cells (Caco-2) and sequential systems (post-transport), under inflammatory and non-inflammatory conditions. Notwithstanding, we demonstrated for the first time the bioactivity of RSV and of its sulfate and glucuronide metabolites in a co-culture towards TNF-α-induced endothelial dysfunction. It was evidenced that the metabolism of endothelial cells as a biological target is not only influenced by polyphenol intervention, but also influenced by the communication between distinct cell lines.

Acknowledgements

The authors acknowledge the financial support of the BOF Special Research Fund (project 01B04212), Hercules Project (AUGE028 and AUGE014) and the Brazilian National Council for Scientific and Technological Development (CNPq) (grant 248460/2013-7 to I.M.T.).

Author's contribution

I.M.T., J.V.C., M.T.B.L. and C.G. contributed to the design of the project, cell experiments and development of the co-culture and the manuscript; G.B.G., S.K., G.S., K.R. and E.C. contributed to the methodology of metabolites identification, cell experiments and UPLC-MS/MS analysis of metabolites. All authors contributed to writing and revision of the manuscript.

Conflict of interest

None declared.

References

[1] Das M, Das DK. Resveratrol and cardiovascular health. Mol Aspects Med 2010;31:503–12.

[2] Libby P. Inflammation in atherosclerosis. Nature 2002;420:19–26.

[3] Hajjar DP, Gotto AM. Biological relevance of inflammation and oxidative stress in the pathogenesis of arterial diseases. Am J Pathol 2013;182:1474–81.

[4] Tabruyn SP, Mémet S, Avé P, Verhaeghe C, Mayo KH, Struman I, Martial JA, Griffioen AW. NF-κB activation in endothelial cells is critical for the activity of angiostatic agents. Mol Cancer Ther 2009;8:2645–54.

[5] Ruiz-Núñez B, Pruimboom L, Dijck-Brouwer DAJ, Muskiet FAJ. Lifestyle and nutritional imbalances associated with Western diseases: causes and consequences of chronic systemic low-grade inflammation in an evolutionary context. J Nutr Biochem 2013;24:1183–1201.

[6] Manach C, Scalbert A, Morand C, Rémésy C, Jiménez L. Polyphenols: food sources and bioavailability. Am J Clin Nutr 2004;79:727–47.

[7] Gresele P, Cerletti C, Guglielmini G, Pignatelli P, Gaetano G, Violi F. Effects of resveratrol and other wine polyphenols on vascular function: an update. J Nutr Biochem 2011;22:201–11.

[8] Saiko P, Szakmary A, Jaeger W, Szekeres T. Resveratrol and its analogs: Defense against cancer, coronary disease and neurodegenerative maladies or just a fad? Mutat Res 2008;658:68–94.

[9] Simão F, Pagnussat AS, Seo JH, Navaratna D, Leung W, Lok J, Guo S, Waeber C, Salbego CG, Lo EH. Pro-angiogenic effects of resveratrol in brain endothelial cells: nitric oxide-mediated regulation of vascular endothelial growth factor and metalloproteinases. J Cereb Blood Flow Metab 2012;32:884–95.

[10] Zhang YQ, Liu YJ, Mao YF, Dong WW, Zhu XY, Jiang L. Resveratrol ameliorates lipopolysaccharide-induced epithelial mesenchymal transition and pulmonary fibrosis through suppression of oxidative stress and transforming growth factor-β1 signaling. Clin Nutr 2015;34:752–60.

[11] Gresele P, Pignatelli P, Guglielmini G, Carnevale R, Mezzasoma AM, Ghiselli A, Momi S, Violi F. Resveratrol, at concentrations attainable with moderate wine consumption, stimulates human platelet nitric oxide production. J Nutr 2008;138:1602–08.

[12] Nagai N, Kubota S, Tsubota K, Ozawa. Resveratrol prevents the development of choroidal neovascularization by modulating AMP-activated protein kinase in macrophages and other cell types. J Nutr Biochem 2014;25:1218–25.

[13] Csiszar A, Smith K, Labinskyy N, Orosz Z, Rivera A, Ungvari Z. Resveratrol attenuates TNF-α-induced activation of coronary arterial endothelial cells: role of NF-κB inhibition. Am. J Physiol Heart Circ Physiol 2006;291:1694–99.

[14] Thiel G, Rossler, OG. Resveratrol stimulates AP-1-regulated gene transcription. Mol Nutr Food Res 2014;58:1402–13.

[15] Storniolo CE, Moreno JJ. Resveratrol metabolites have an antiproliferative effect on intestinal epithelial cancer cells. Food Chem 2012;134:1385–91.

[16] Polycarpou E, Meira LB, Carrington S, Tyrrell E, Modjtahedi H, Carew MA. Resveratrol 3-O-D-glucuronide and resveratrol 4-O-D-glucuronide inhibit colon cancer cell growth: Evidence for a role of A3 adenosine receptors, cyclin D1 depletion, and G1 cell cycle arrest. Mol Nutr Food Res 2013;57:1708–17.

[17] Maaser C, Schoeppner S, Kucharzik T, Kraft M, Schoenherr E, Domschke W, Luegering N. Colonic epithelial cells induce endothelial cell expression of ICAM-1 and VCAM-1 by a NF-kappaB-dependent mechanism. Clin Exp Immunol 2001;124:208–13.

[18] Kuntz S, Asseburg H, Dold S, Römpp A, Fröhling B, Kunz C, Rudloff S. Inhibition of low-grade inflammation by anthocyanins from grape extract in an in vitro epithelial-endothelial co-culture model. Food Funct 2015;4:1136–49.

[19] Notarnicola M, Pisanti S, Tutino V, Bocale D, Rotelli MT, Gentile A, Memeo V, Bifulco M, Perri E, Caruso MG. Effects of olive oil polyphenols on fatty acid synthase gene expression and activity in human colorectal cancer cells. Genes Nutr 2011;6:63–9.

[20] Goldberg DM, Yan J, Soleas GJ. Absorption of three wine-related polyphenols in three different matrices by healthy subjects. Clin Biochem 2003;36:79–87.

[21] Walle T, Hsieh F, Delegge MH, Oatis JE, Walle UK. High absorption but very low bioavailability of oral resveratrol in humans. Drug Metab Dispos 2004;32:1377–82.

[22] Boocock DJ, Faust GE, Patel KR, et al. Phase I dose escalation pharmacokinetic study in healthy volunteers of resveratrol, a potential cancer chemopreventive agent. Cancer Epidemiol Biomarkers Prev 2007;16:1246–52.

[23] Calatayud M, Gimeno J, Vélez D, Devesa V, Montoro R. Characterization of the intestinal absorption of arsenate, monomethylarsonic acid, and dimethylarsinic acid using the caco-2 cell line. Chem Res Toxicol 2010;23:547–56.

[24] Gonzales GB, Raes K, Coelus S, Struijs K, Smagghe G, Van Camp J. Ultra (high)-pressure liquid chromatography–electrospray ionization-time-of-flight-ion mobility-high

definition mass spectrometry for the rapid identification and structural characterization of flavonoid glycosides from cauliflower waste. J Chromatogr A 2014;1323:39-48.

[25] Chiesi C, Fernandez-Blanco C, Cossignani L, Font G, Ruiz MJ. Alternariol-induced cytotoxicity in Caco-2 cells. Protective effect of the phenolic fraction from virgin olive oil. Toxicon 2015;93:103–11.

[26] Li A, Varney ML, Singh RK. Expression of interleukin 8 and its receptors in human colon carcinoma cells with different metastatic potentials1. Clin Cancer Res;7:3298–3304.

[27] Lai Y, Shen Y, Liu XH, Zhang Y, Zeng Y, Liu YF. Interleukin-8 induces the endothelial cell migration through the activation of phosphoinositide 3-kinase-Rac1/RhoA pathway. Int J Biol Sci 2011;7:782–791.

[28] Harrison DJ, Gongora MC. Oxidative stress and hypertension. Med Clin N Am 2009;93:621–35.

[29] Claude S. Boby C, Rodriguez-Mateos A, Spencer JPE, Gérard N, Morand C, Milenkovic D. Flavanol metabolites reduce monocyte adhesion to endothelial cells through modulation of expression of genes via p38-MAPK and p65-Nf-kB pathways. Mol Nutr Food Res 2014;58:1016–27.

[30] Das S, Alagappan VKT, Bagchi D, Sharma HS, Maulik N, Das DK. Coordinated induction of iNOS–VEGF–KDR–eNOS after resveratrol consumption: A potential mechanism for resveratrol preconditioning of the heart. Vascul Pharmacol 2005;42:281–89.

[31] Kim JJ, Lee SB, Park JK, Yoo YD. TNF-α-induced ROS production triggering apoptosis is directly linked to Romo1 and Bcl-XL. Cell Death Differ 2010;17:1420–34.

[32] Palomer X, Capdevila-Busquets E, Álvarez-Guardia D, Barroso E, Pallàs M, Camins A, Davidson MM, Planavila A, Villarroya F, Vázquez-Carrera M. Resveratrol induces nuclear factor-κB activity in human cardiac cells. Int J Cardiol 2013;167:2507–16.

[33] Zhang J, Peng B. In vitro angiogenesis and expression of nuclear factor *κβ* and VEGF in high and low metastasis cell lines of salivary gland Adenoid Cystic Carcinoma. BMC Cancer 2007;7:95.

[34] Penumathsa SV, Koneru S, Samuel SM, Maulik G, Bagchi D, Yet SF, Menon VP, Maulik N. Strategic targets to induce neovascularization by resveratrol in hypercholesterolemic rat myocardium: Role of caveolin-1, endothelial nitric oxide synthase, hemeoxygenase-1, and vascular endothelial growth factor. Free Radical Biol Med 2008;45:1027–34.

[35] Ladurner A, Schachner D, Schueller K, Pignitter M, Heiss EH, Somoza V, Dirsch VM. Impact of trans-resveratrol-sulfates and -glucuronides on endothelial nitric oxide synthase activity, nitric oxide release and intracellular reactive oxygen species. Molecules 2014;19:16724–36.

[36] Menet MC, Cottart CH, Taghi M, Nivet-Antoine V, Dargère D, Vibert F, Laprévotea O, Beaudeuxc J-L. Ultra high performance liquid chromatography-quadrupole-time of flight

analysis for the identification and the determination of resveratrol and its metabolites in mouse plasma. Anal Chim Acta 2013;761:128–36.

Figure captions

Figure 1. Representative MS/MS^{E} chromatograms of the transported fraction after 24 h incubation of Caco-2 cells treated with RSV. Total ion chromatogram (A) of RSV and its metabolites: 1 = *trans*-resveratrol-4'-*O*-*β*-glucuronide, 2 = *trans*-resveratrol-4'-sulfate, 3 = *trans*-resveratrol-3-sulfate, 4 = *trans*-resveratrol-3-*O*-*β*-glucuronide, 5 = *trans*-resveratrol. Extracted ion chromatogram of resveratrol (*m/z* 227.07) and its sulfate (*m/z* 307.03) (B) and glucuronide (*m/z* 403.11) (C) metabolites.

Figure 2. Mitochondrial activity of endothelial cells at 4 h (A) and 24 h (B) in response to RSV treatment in co-culture (black bars), sequential (dark grey bars) and standard (light grey bars) systems, under TNF-*α*-induced inflammatory and non-inflammatory conditions, expressed as percentage towards untreated cells without TNF-*α* addition. Results are expressed as percentage of the control condition that did not receive a RSV or TNF-*α* treatment. Data represent the mean ± SEM, three measurements in triplicates, in three independent experiments. * and ** indicate significant differences ($p<0.05$ and $p<0.001$, respectively) compared to the respective control sample without RSV treatment; and $^{\#}$ and $^{\#\#}$ indicate significant differences ($p<0.05$ and $p<0.001$, respectively) compared to the respective control sample without TNF-*α* treatment.

Figure 3. Effect of RSV and metabolites on NO production at 4h (A) and 24h (B) under TNF-α-induced inflammation and non-inflammatory condition, expressed as percentage towards untreated cells without TNF-α addition. Data expressed as mean ± SEM of triplicates, in three independent experiments. * and ** indicate significant differences ($p<0.05$ and $p<0.001$, respectively) compared to the respective control sample without RSV treatment; and $^{\#}$ and $^{\#\#}$ indicate significant differences ($p<0.05$ and $p<0.001$, respectively) compared to the respective control sample without TNF-α treatment.

Figure 4. Changes in intracellular ROS levels in response to RSV and metabolites at 4 h (A) and 24 h (B), expressed as percentage towards untreated cells without TNF-α addition. Data are expressed as mean ± SEM of three measurements in triplicates, in three independent experiments. * and ** indicate significant differences ($p<0.05$ and $p<0.001$, respectively) compared to the respective control sample without RSV treatment; and $^{\#}$ and $^{\#\#}$ indicate significant differences ($p<0.05$ and $p<0.001$, respectively) compared to the respective control sample without TNF-α treatment.

Figure 5. Secretion of proinflammatory chemokines and vascular endothelial growth factor after 4 h (T4) and 24 h (T24) exposure to RSV in the co-culture, expressed as percentage towards untreated cells without TNF-α addition. A) IL-8; B) VEGF; C) ICAM-1. Data represent the mean ± SEM, three measurements in triplicates, in three independent experiments. * and ** indicate significant differences ($p<0.05$ and $p<0.001$, respectively) compared to the respective control sample without RSV treatment; and $^{\#}$ and $^{\#\#}$ indicate significant differences ($p<0.05$ and $p<0.001$, respectively) compared to the respective control sample without TNF-α treatment.

692

693

694

Table(s)

Table 1. Modifications of RSV and metabolites identified by UPLC-ESI-HDMS/MS^2 after metabolism and transport by Caco-2 cells.

Identified compound	Molecular formula	Rt (min)	Molecular mass	Detected *m/z*	MS/MS fragment	Neutral loss	Modification
(1) *Trans*-Resveratrol-4'-*O*-*β*-glucuronide	C20H20O9	15.85	404.11	403.11	227.07	176	Glucuronide conjugation
(2) *Trans*-Resveratrol-4'-sulfate	C14H12O6S	17.23	308.04	307.03	227.07	80	Sulfate conjugation
(3) *Trans*-Resveratrol-3-sulfate	C14H12O6S	20.19	308.04	307.03	227.07	80	Sulfate conjugation
(4) *Trans*-Resveratrol-3-*O*-*β*-glucuronide	C20H20O9	20.58	404.11	403.11	227.07	176	Glucuronide conjugation
(5) *Trans*-Resveratrol	C14H12O3	23.53	228.07	227.07	-	0	-

Figure(s)

Click here to download high resolution image

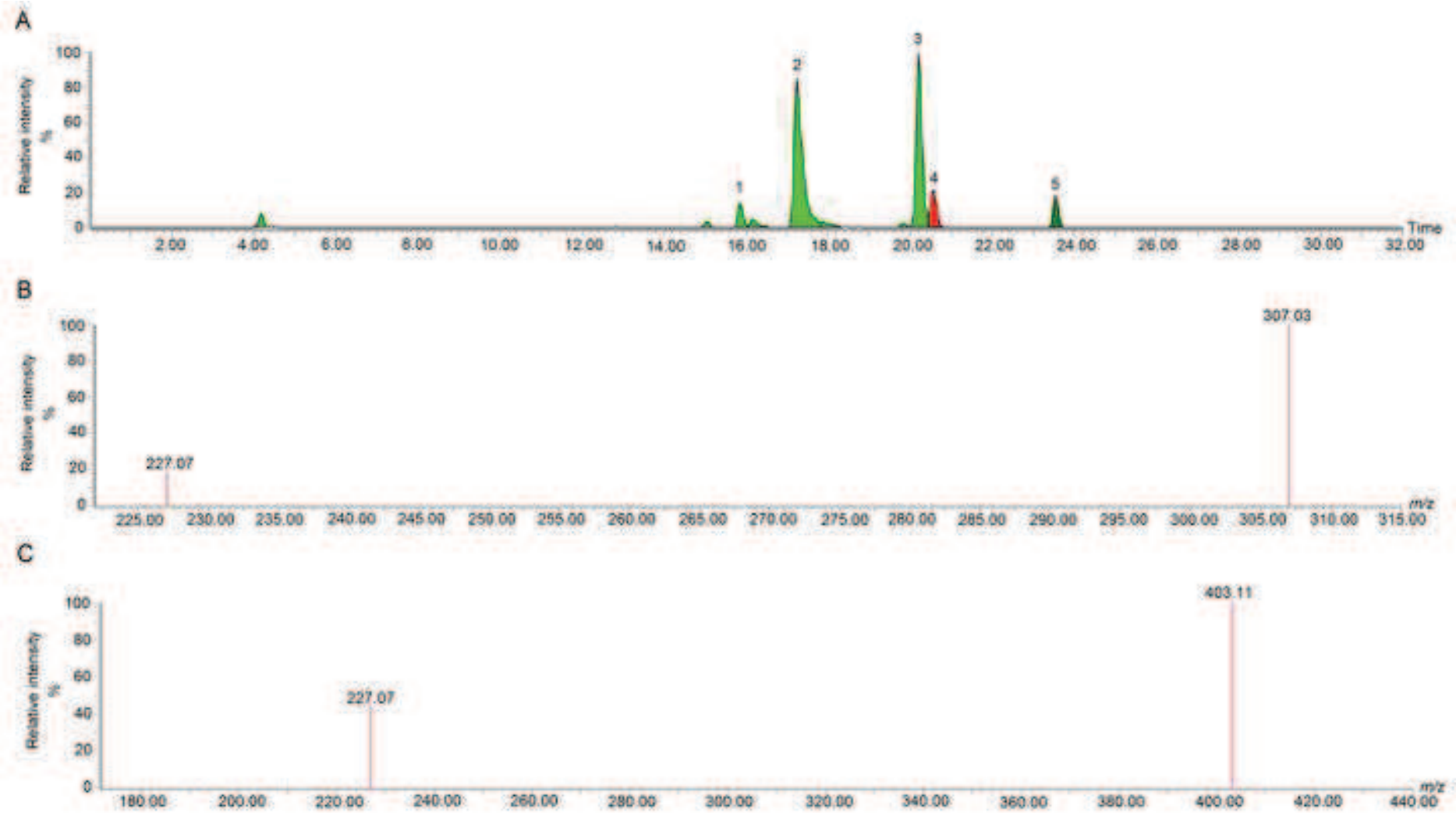

Figure(s)

Click here to download high resolution image

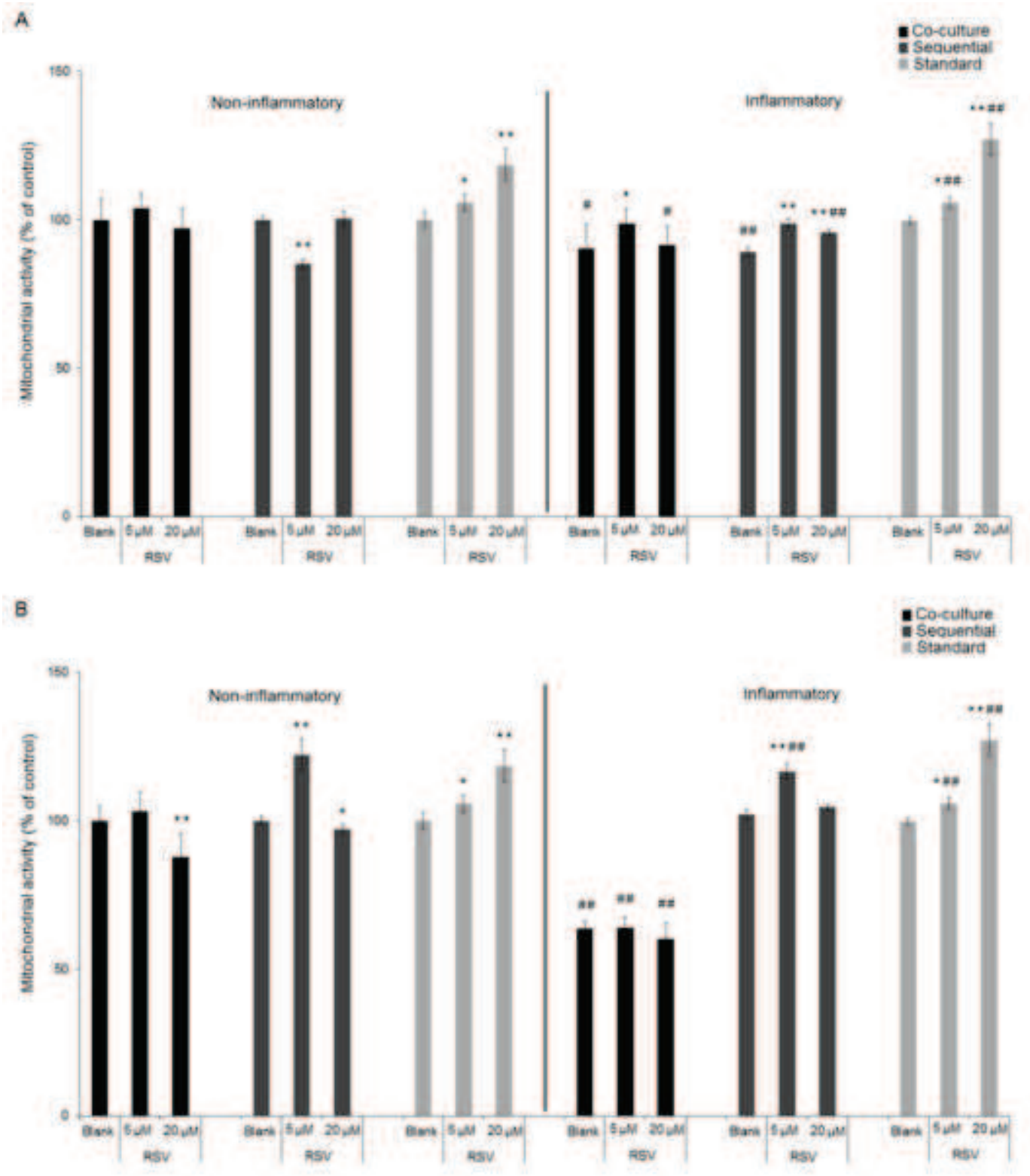

Figure(s)

Click here to download high resolution image

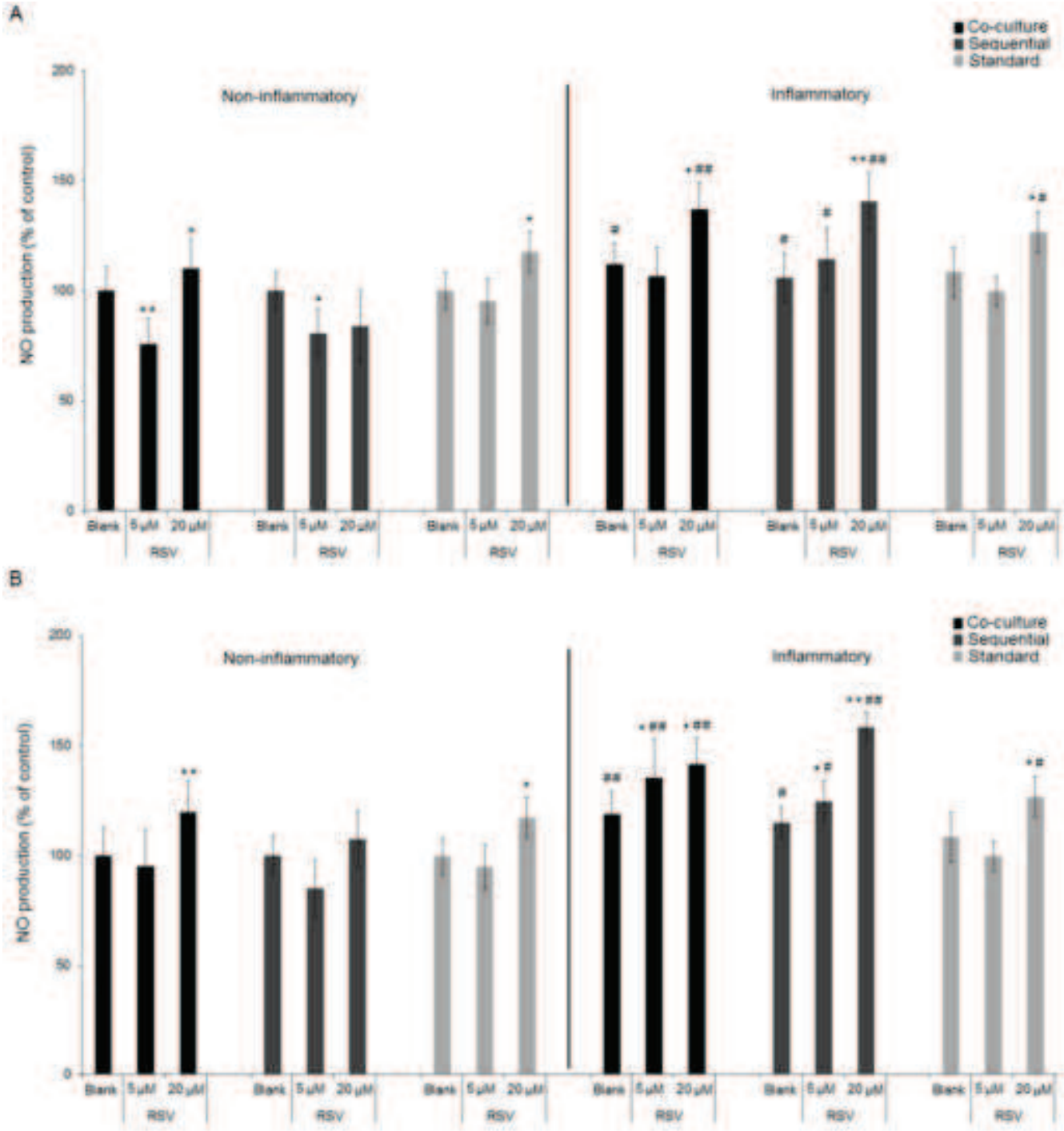

Figure(s)

Click here to download high resolution image

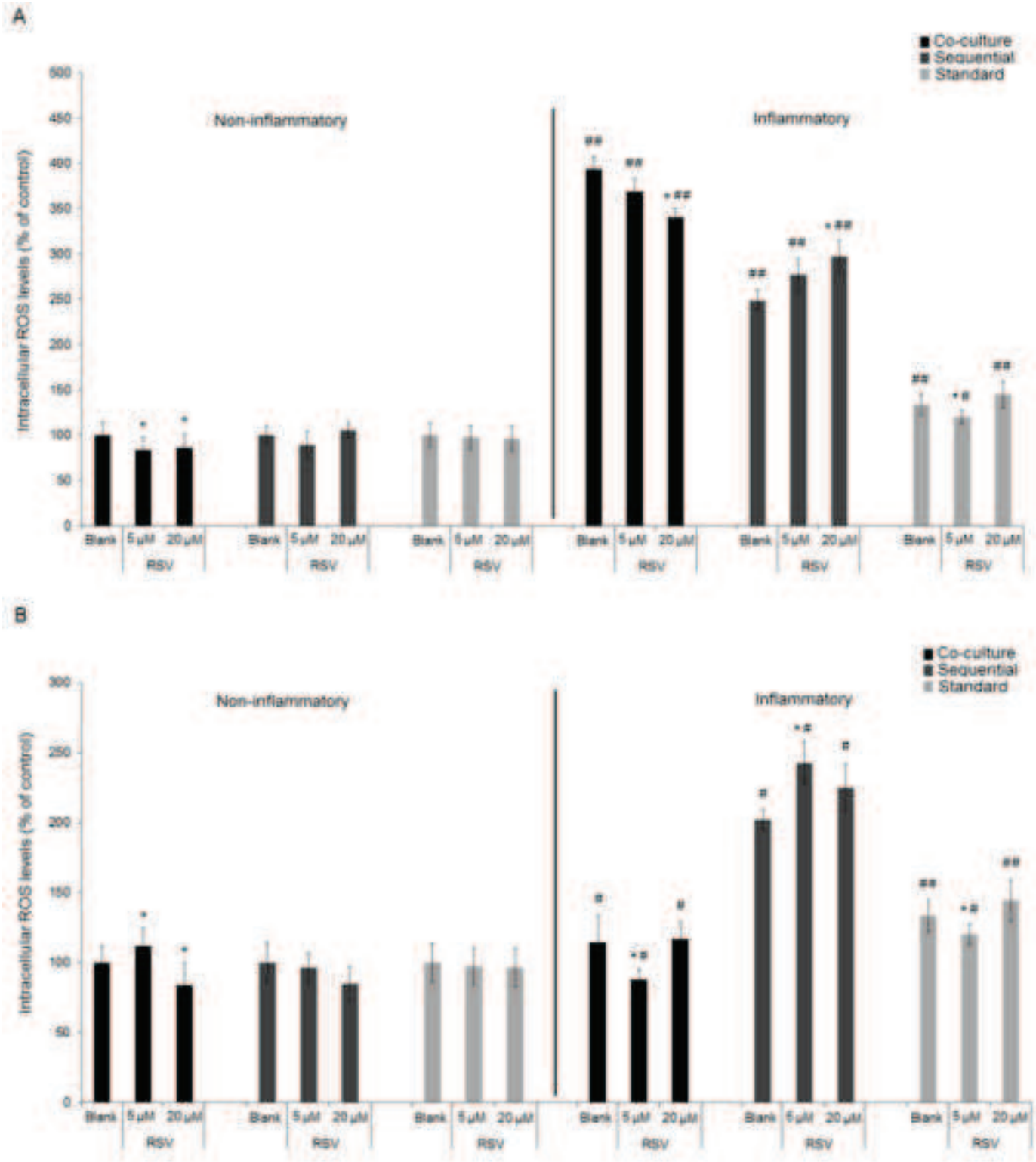

Figure(s)

Click here to download high resolution image